



Natural attrition and growth frequency variations of stalagmites in southwest Sulawesi over the past 530,000 years



Nick Scroxtan^{a,*}, Michael K. Gagan^a, Gavin B. Dunbar^b, Linda K. Ayliffe^a, Wahyoe S. Hantoro^c, Chuan-Chou Shen^d, John C. Hellstrom^e, Jian-xin Zhao^f, Hai Cheng^{g,h}, R. Lawrence Edwards^g, Hailong Sun^{d,i}, Hamdi Rifai^j

^a Research School of Earth Sciences, The Australian National University, Canberra, ACT 0200, Australia

^b Antarctic Research Centre, Victoria University of Wellington, Wellington 6140, New Zealand

^c Research Centre for Geotechnology, Indonesian Institute of Sciences, Bandung 40135, Indonesia

^d High-Precision Mass Spectrometry and Environmental Change Laboratory (HISPEC), Department of Geosciences, National Taiwan University, Taipei 10617, Taiwan, ROC

^e School of Earth Sciences, University of Melbourne, Parkville, VIC 3010, Australia

^f School of Earth Sciences, University of QLD, Brisbane, QLD 4072, Australia

^g Department of Earth Sciences, University of Minnesota, Minneapolis, MN 55455, USA

^h Institute of Global Environmental Change, Xi'an Jiatong University, Xi'an 710049, China

ⁱ State Key Laboratory of Environmental Geochemistry, Institute of Geochemistry, Chinese Academy of Sciences, Guiyang 550002, China

^j Department of Physics, State University of Padang, Padang 25131, Indonesia

ARTICLE INFO

Article history:

Received 5 May 2015

Received in revised form 14 October 2015

Accepted 20 October 2015

Available online 27 October 2015

Keywords:

Indonesia

Stalagmite growth

U–Th dating

Palaeoclimatology

Australasian monsoon

ABSTRACT

Previous studies have analysed the age distributions of stalagmites harvested from multiple caves and inferred important palaeoclimate changes that explain stalagmite growth phases. However, stalagmites may grow over tens of thousands of years; thus, they are irreplaceable. The value of speleothems to science must be weighed against their potential and current aesthetic and cultural value. In this study, we show that some palaeoclimate information can be extracted from a cave system without the removal of stalagmites. Our case study is based on basal U–Th dates for 77 individual stalagmites from thirteen caves located in and around Bantimurung-Bulusaraung National Park, southwest Sulawesi, Indonesia. The stalagmites grew during discrete intervals within the last ~530,000 years, and an analysis of their age distribution shows a first-order exponential decrease in the number of older stalagmites surviving to the present day. Further, this exponential relationship is observed in stalagmite populations around the world and is therefore likely to be a general cave phenomenon. Superimposed on the first-order exponential age distribution in southwest Sulawesi are positive anomalies in stalagmite growth frequency at 425–400, 385–370, 345–335, 330–315, 160–155, 75–70 and 10–5 ka, which are typically coincident with wet periods on Borneo. To explain this distribution, we present a simple model of stalagmite growth and attrition. A first-order trend is controlled by processes intrinsic to karst systems that govern the natural attrition of stalagmites. These processes are nearly constant over time and result in the observed exponential relationship of stalagmite basal ages. Second-order variation is controlled by changes in the rate of stalagmite generation caused by fluctuating climates, which is a well-known concept in the speleothem literature. Removal of the exponential baseline allows for better assessment of relative peak heights and basic palaeoclimate information to be inferred. Importantly, the first- and second-order growth frequency variations can be characterised using basal stalagmite ages only, without the removal of stalagmites, thereby helping reduce the impact of scientific sampling on the cave environment.

© 2015 Elsevier B.V. All rights reserved.

1. Introduction

The appeal of stalagmites as a long-term, precisely dated continental palaeoclimate archive has led to a proliferation of research in recent years (e.g., Wang et al., 2001; Genty et al., 2003; Cruz et al., 2005;

Meckler et al., 2012; Jo et al., 2014). However, the removal of stalagmites from caves for scientific research can be a mixed blessing for local communities: palaeoclimate reconstructions from geochemical analyses of stalagmites can improve knowledge and adaptation strategies for climatic events and changes. But there is also significant monetary value in preserving the aesthetic value of cave systems in their natural state for tourism, which provides direct financial benefits to local communities. Recreational use of non-show caves also provides indirect benefits to local communities. Caves may represent important

* Corresponding author at: Research School of Earth Sciences, Building 142, Mills Road, The Australian National University, Acton, ACT 2601, Australia. Tel.: +61 261253406.
E-mail address: Nick.Scroxtan@anu.edu.au (N. Scroxtan).

centres of local cultural heritage, such as religious spaces (e.g., Batu Caves, Malaysia). Therefore, caves of all types must be protected, and scientists should match the custodial care provided by the caving communities in preserving their natural conditions (Baker and Genty, 1998; Calaforra and Fernandez-Cortés, 2003; Cigna and Burri, 2012; Verheyden and Genty, 2013; Šebela and Turk, 2014).

In some cases stalagmites have grown continuously for tens of thousands of years; thus, they are irreplaceable and can be considered a finite resource. However, the value of stalagmites is uncertain because they are highly valuable in terms of their value to science and tourism and worthless because they have little or no direct economic value. Thus, questions of how to manage the competing interests of scientific research versus the present and the future value of stalagmites in their original locations remain an issue.

In this study, we show that these two ideals can be reconciled by extracting palaeoclimate information from a cave system without the removal of stalagmites, thus retaining the intrinsic value of the cave. We follow in the footsteps of stalagmite dating studies that reconstruct past climates using the age distributions of stalagmites harvested from caves (e.g. Hennig et al., 1983; Gordon et al., 1989; Baker et al., 1993; Ayliffe et al., 1998; Hercmann, 2000; Wang et al., 2004; Vaks et al., 2006, 2010, 2013; Williams et al., 2010; Jo et al., 2014). However, our approach utilises the ages of low-impact mini-cores extracted in situ from the bases of stalagmites, thus eliminating the need to remove specimens from their original locations. The focus of this work is two-fold: (1) quantify the age distribution of populations of stalagmites to help improve sampling strategies for scientific research; and (2) determine if palaeoclimate information can be gained by analysing the growth frequency variations in populations of stalagmites.

Although the removal of stalagmites cannot be completely avoided using this approach (i.e., for isotopic and trace element studies), our approach reduces the overall number of stalagmites required for collection and provides an assessment of periods of time favourable to stalagmite growth. Where stalagmites cannot be removed because of cultural significance, this “first pass” may provide the only source of palaeoclimate information.

1.1. Environmental context of stalagmites

The simplest palaeoclimate proxy that can be provided by a stalagmite is its presence (Gascoyne et al., 1983). Carbonate stalagmite growth is generated by in-cave CO₂ degassing that triggers the precipitation of calcium carbonate from a solution to an in-cave surface. For the occurrence of stalagmite formation, there must be a solvent (liquid water) and a solute (typically limestone or dolomite). High concentrations of dissolved CO₂ in percolating waters are required for the dissolution of calcium carbonate host rocks and typically form via root and microbial respiration in the soil above the karst; however, they may also form by dissolution of soluble acidic minerals (Atkinson, 1983; Spötl and Mangini, 2007). The presence of a stalagmite is therefore dependent (in most cases) on the presence of soil and sufficient liquid water, which represents the simplest type of palaeoclimate information.

In an early study, Geyh (1970) used radiocarbon dating to compile histograms of speleothem growth density over the last 50 ka. Ayliffe et al. (1998) produced a 500,000-year precipitation record for south-eastern Australia using speleothem growth as an indicator of wetter climates. Here, stadials and cool interstadials correspond to greater effective precipitation because of reduced evaporation rates. Similarly, Wang et al. (2004) found that periods of speleothem growth in a semi-arid region of Brazil correlated with local maxima in autumn insolation and millennial-scale Heinrich events over the last 200,000 years. They attributed speleothem growth to increased rainfall during southward displacements of the InterTropical Convergence Zone (ITCZ). Vaks et al. (2006, 2010) mapped isohyets (lines of equal rainfall) in southern Israel to reveal wet periods in the area over the last

two glacial cycles. Holocene speleothems in the region only grow where there is more than 300–350 mm of annual rainfall, and the age distribution of older stalagmites provides an estimate of the location of the 200–275 mm isohyet (Vaks et al., 2006). Vaks et al. (2013) repeated this experiment on Siberian stalagmites and inferred that periods of permafrost thawing allowed for flowing water and speleothem growth.

In wetter climatic settings where speleothem growth may not cease because of climate variability, the frequency distribution of stalagmites can yield similarly important information on climates of the past. Gordon et al. (1989) used 341 U–Th dates on stalagmites from the United Kingdom to constrain the timing of ten interstadials over the past 220,000 years. Hennig et al. (1983) compiled a global data set of 805 speleothem and travertine dates that showed high numbers of stalagmites during the last interglacial. Baker et al. (1993) compiled 520 U–Th dates to show that speleothem growth frequency is highly correlated with the marine oxygen isotope record over the past 160 kyr. In this case, the frequency of growing stalagmites was interpreted as resulting from a combination of changes in mobile groundwater supply and temperature modulating soil CO₂ production.

1.2. Conservation of stalagmites

The distribution of speleothems over time must be understood to improve our sampling “footprint” — only those stalagmites strictly necessary for scientific progress should be collected. Certain research groups take the commendable approach of only removing stalagmites that have been broken naturally (McDonnell, 2013), but this is rarely practicable for the production of a long and continuous palaeoclimate record.

As an alternative, Frappier (2008) outlined a four-step approach for identifying stalagmites that are likely to yield accurate proxy records of the desired palaeoclimate variable with a high signal-to-noise ratio. This method involves a step-wise screening process that gradually decreases in scale from the karst region to the cave and stalagmite required for analysis. Data gathered during this process, such as monitoring the geochemistry of cave drip waters, provide important additional information for the interpretation of geochemical proxies.

Stalagmites that satisfy all of the above criteria may still be rejected on ethical grounds if they are aesthetically important to cave tourism or the cultural heritage of the site. It is also possible, in certain cases, to re-install stalagmites in their cave of origin in the event that they are not suitable for palaeoclimate study or after analysis if the stalagmites are cored rather than slabbed (Dorale et al., 1992). For example, high-resolution X-ray computed tomography can be used in the laboratory to assess the integrity of internal structures before opening the stalagmite (Mickler and Ketcham, 2004; Walczak et al., 2015). If the sample is suitable for geochemical analysis, this step helps to reduce wastage caused by misplaced cuts and improves results by ensuring that the central growth axis is accurately sampled.

Fairchild and Baker (2012) provide examples of good practice and suitable protocols for the archiving and protection of speleothem materials in the laboratory and storage using techniques largely borrowed from the archaeological community (Brown, 2011). Finally, resampling previously explored caves should be avoided by sharing archived material and storing data in online repositories, such as that of NOAA or the PANGAEA archive. The archived half of a speleothem should always be kept pristine so that non-destructive analyses can be conducted in the future.

In this study we propose an additional method by which speleothem researchers can minimise their impacts on cave systems. We utilise only the ages of minimally destructive mini-cores extracted in situ from the bases of stalagmites to recreate previous studies of speleothem growth history (e.g., Ayliffe et al., 1998; Vaks et al., 2010) without using data that require wholesale collection of stalagmites.

2. Materials and methods

Our case study is based on U–Th dates for 77 individual stalagmites drilled in situ in 2009 and 2011 in caves in the tower karst terrain of southwest Sulawesi. This study utilises basal cores from all stalagmites believed to be suitable for further palaeoclimate analysis found in 25 different caves located in and around Bantimurung-Bulusaraung National Park in the Maros Regency, South Sulawesi (4°54'S 119°45'E, Fig. 1a). In 12 of these caves, no specimens were found. Stalagmites were collected from the thirteen decorated caves. In the less well decorated caves this resulted in the dating of all available specimens. In more well decorated caves as many stalagmites were sampled as possible, with priority given to those likely to yield good palaeoclimate information.

An initial reconnaissance expedition to southwest Sulawesi in 2009 collected only stalagmites that had already fallen, as well as

reconnaissance dates from upright and in place stalagmites for U–Th dating. The basal ages of the fallen stalagmites collected are included in this study. The second field season in 2011 involved collecting only samples of known age that had been previously cored and the ages matched the scientific interval of interest, along with further drilling of reconnaissance dates.

The tower karst of Bantimurung-Bulusaraung National Park is at the southern end of the Tonasa Limestone Formation, an isolated platform sequence of packstones and wackestones that is dominated by photic zone benthic foraminifera (Wilson, 2000) (Fig. 2). The carbonate sequence was deposited between the Middle Eocene and Middle Miocene (Wilson and Bosence, 1996; Wilson and Moss, 1999). The area is bounded by Quaternary alluvium deposits to the west and Middle to Late Miocene volcanoclastic deposits to the east, although it is now volcanically inactive (Wilson and Bosence, 1996).

The island of Sulawesi is surrounded by the West Pacific Warm Pool, where average annual sea surface temperatures (SSTs) exceed 28 °C (Fig. 1a) and precipitation is dominated by the Australasian monsoon (Fig. 1b). The caves lie in the western rain shadow of the southern Sulawesi highlands and receive little rainfall in the winter (dry season) from the southeast monsoon. As a result, southwest Sulawesi receives ~70% of its annual rainfall during the austral summer from the northwesterly monsoon. There is a pronounced decrease in rainfall over southwest Sulawesi during El Niño years due to changes in Walker Circulation (Dai and Wigley, 2002).

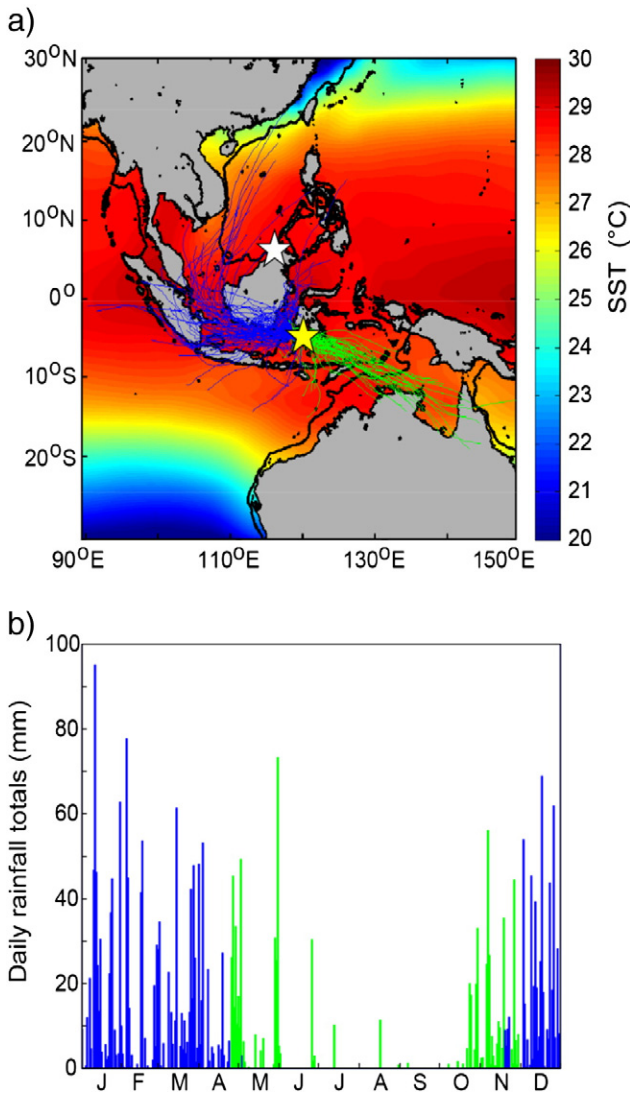


Fig. 1. Location and modern climate of the study area. a) The yellow star shows the study caves in the Maros region of southwest Sulawesi and the white star shows the location of caves in north Borneo discussed in the text. Green and blue lines are the 96-hour back trajectory air flow pathways that delivered rainfall to the Maros region during 2011 from westerlies (blue) and easterlies (green). b) Distribution of total daily rainfall amounts in 2011 with colour-coding as before. Rain days were extracted from the NASA Tropical Rainfall Measuring Mission (TRMM) satellite daily (defined by UTC) estimates of rainfall between 5.01–5.02°S and 119.68–119.69°E using the Giovanni programme (Acker and Leptoukh, 2007). Trajectories were calculated for all TRMM rain days using Global Data Assimilation System (GDAS) data from the NOAA HYSPLIT model of air parcels at 500 m altitude arriving at 5.019°S, 119.686°E at 12:00 UTC (Draxler and Rolph, accessed, 2012).

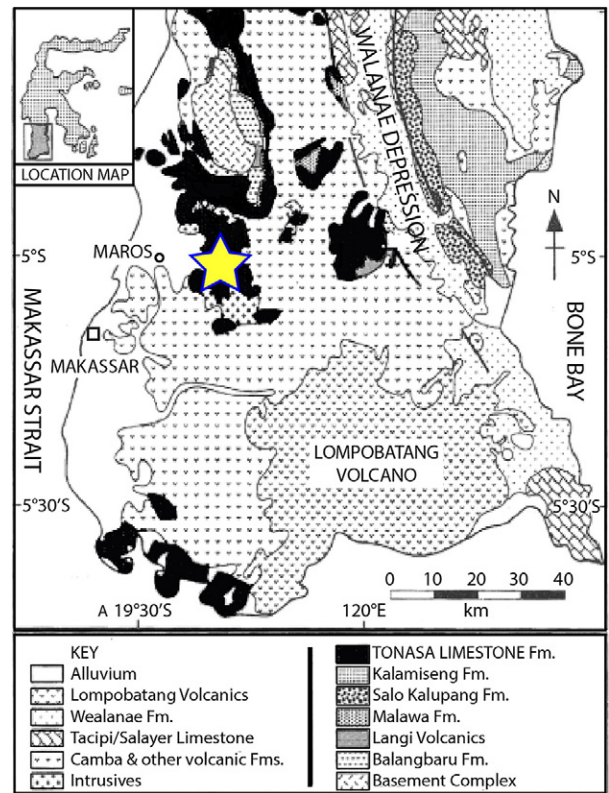


Fig. 2. Geological map of southwest Sulawesi highlighting the Tonasa Limestone Formation (black) with the cave sites in the Maros region (yellow star). Adapted from Wilson and Bosence (1996).

2.1. Stalagmite mini-coring

Mini-coring is the process of drilling into a stalagmite to extract either a core sample (using a coring barrel) or a powder sample (using a solid drill bit) from close to the central growth axis near the base of the stalagmite. Coring has the advantage of allowing for direct visual analysis of the speleothem calcite, which can provide more accurate proximal determinations of the date for the central growth axis (indicated by horizontal laminations) and an assessment of the quality of the material. In this study, we used a technique similar to that outlined for small diameter cores by Spötl and Matthey (2012). Briefly, a hand-held 36-volt (or 18-volt) battery-powered DeWalt drill was used to drive a diamond-tipped core barrel with an internal diameter of 16 mm. Water was applied at moderate pressure to remove loose material and cool the core barrel.

The advantage of collecting powder samples from the bases of stalagmites is that they are quicker to drill, require no water for flushing and are more discreet, leaving a smaller hole. However, they do not allow for visual inspection of calcite quality. Powder samples are obtained by a two-step drilling process. First, a 10 mm-diameter solid masonry drill bit is used to clear material from a hole to within ~1 cm of the centre of a stalagmite, assuming symmetrical growth. The hole is then flushed with water to remove any remaining powder. A clean drill bit (of the same diameter) is deployed through a protective clear plastic sleeve inserted into the hole. This second drilling step removes approximately 1 cm³ of stalagmite material. The extracted powder is drawn into the plastic sleeve automatically and then transferred to a plastic zip lock bag. Some plastic may be removed from the inside of the sleeve by the drill but are easily recognisable against the powder. The extracted powder/chips are then be returned to the lab and dated. Powders and chips can both be used for X-ray diffraction and $\delta^{18}\text{O}$ analysis to further constrain the suitability of the dated specimens for collection.

Additional material can be collected from either the top of the stalagmite or outside of the mini-core to constrain the entire growth interval; however, this procedure relies on the assumption that there are no growth hiatuses contained within. A full assessment of the entire growth interval is only possible with the removal of the stalagmite from the cave, which this study is designed to avoid. Our experience shows that only a small amount of additional information is gained from top dating so the use of basal dates to determine the onset of stalagmite growth is the most robust method of determining wet and dry periods whilst minimising damage to the specimen and cave environment.

2.2. U–Th dating

The basal U–Th ages of 77 stalagmites were determined using multi-collector inductively coupled plasma mass spectrometry (MC-ICP-MS) at the National Taiwan University (35 samples), University of Melbourne (27 samples), University of Queensland (9 samples) and University of Minnesota (6 samples). The MC-ICP-MS analytical protocols are summarised in Hellstrom (2003, 2006) and Shen et al. (2002; 2012) and use new half-lives obtained from Cheng et al. (2013): ²³⁰Th (75,584 ± 110 yrs) and ²³⁴U (245,620 ± 260 yrs).

Stratigraphical constraint modelling (Hellstrom, 2006) of 34 U–Th dates for a 40,000-year stalagmite $\delta^{18}\text{O}$ record for the study area was used to calculate an area-specific detrital (²³⁰Th/²³²Th)_{initial} value of 3.00 ± 0.75 (Krause pers. comm.). This detrital (²³⁰Th/²³²Th)_{initial} value was applied to all of the basal U–Th ages to correct for detrital ²³⁰Th contamination and standardise the outputs from the different laboratories. We consider this value to be more appropriate for the stalagmite U–Th ages presented here compared with the generic crustal value of 0.82 ± 0.41, which is used when no other information is available. An isochron determination should be possible from a mini-core if individual layers can be traced. Detrital ²³⁰Th contamination of the Bantimuring

stalagmite mini-core and powder samples is variable and resulted in 2 σ age precisions ranging from ±0.3% to +2500%/–3000% (median of 2.5%, 76% of samples less than 5% error) (Supplementary Table S1).

3. Results

The basal U–Th ages of the 77 stalagmites span the last five glacial–interglacial cycles, with the oldest stalagmite dating to 529 ± 30 ka (thousand years before the present, where present is AD 1950) (Table S1). In the first instance, all of the dated samples are included in our results regardless of the amount of ²³⁰Th contamination and the size of the resulting age errors to avoid introducing bias. Under this scenario, the number of younger stalagmites greatly exceeds the number of older stalagmites, and the distribution of stalagmites over the last ~530 kyr approximates an exponential curve (Fig. 3a).

To improve the accuracy of the data set, we combined basal ages to avoid over-representation of stalagmite populations that have attracted attention as a result of their scientifically interesting age span and because a single drip flow route may result in multiple stalagmites. Therefore, any specimens from the same cave with ages overlapping within a 1 sigma confidence limit are combined to form one data point. This is achieved by Gaussian fusion, a maximum likelihood estimate for two Gaussian distributions (Table 1). In certain cases, ages may overlap with two separate non-overlapping dates. For this scenario, the

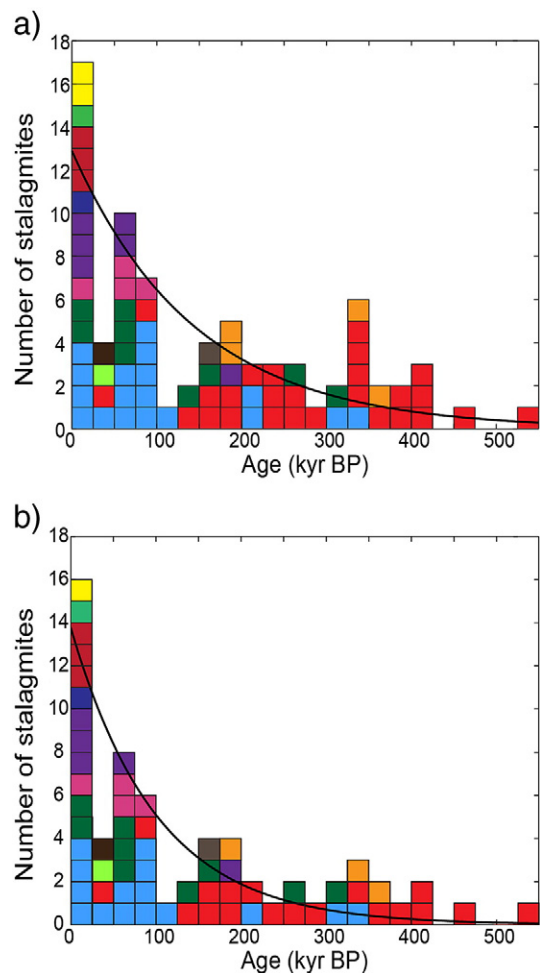


Fig. 3. Distribution of mean stalagmite ages over the last ~530 kyr in 13 caves in southwest Sulawesi. a) Ages of all 77 stalagmites that were sampled. b) Ages of the adjusted set of 63 stalagmites after accounting for potential duplication of single drip-sites. Each individual cave is represented by a different colour. Black curves show that a best-fit exponential relationship works as well for histogram data as it does for the probability density functions used elsewhere in this study.

Table 1

Summary of stalagmite U–Th ages. To avoid over-representing stalagmite populations in the same cave with overlapping stalagmite ages ($\pm 1\sigma$), ages have been combined by Gaussian summation (grey shading). In some instances, samples with large errors are used in the summation of more than one combined age. Combined ages are identified with the letter H (e.g., ML-H1). Powder samples are identified with the letter P (e.g., MD-P1). Ages are reported as thousands of year before present (ka), where the present is defined as AD 1950. Full U–Th results are in Supplementary Table S1.

Original stalagmites (n = 77)		Adjusted stalagmites (n = 63)		Original stalagmites (n = 77)		Adjusted stalagmites (n = 63)	
Sample	Corr. age $\pm 1\sigma$	Sample	Age $\pm 1\sigma$	Sample	Corr. age $\pm 1\sigma$	Sample	Age $\pm 1\sigma$
ML-2	0 \pm 10			MB-M2	129.6 \pm 1.9	MB-M2	129.6 \pm 1.9
MD-P1	0.59 \pm 0.76	MD-P1	0.59 \pm 0.76	MC-4	133.37 \pm 0.71	MC-4	133.37 \pm 0.71
ME-2	1.12 \pm 0.39	ME-2	1.12 \pm 0.39	MB-P6	150.1 \pm 4.6	MB-P6	150.1 \pm 4.6
MA-M3	2.52 \pm 0.94	MA-M3	2.52 \pm 0.94	MM-1	156.92 \pm 0.33	MM-1	156.92 \pm 0.33
MA-5	5.117 \pm 0.054	MA-5	5.117 \pm 0.054	MC-3	158.3 \pm 1.0	MC-3	158.3 \pm 1.0
ML-1	5.39 \pm 0.22	ML-H1	5.38 \pm 0.22	MB-P5	160.9 \pm 3.9	MB-P5	160.9 \pm 3.9
MA-4	6.381 \pm 0.071	MA-4	6.381 \pm 0.071	MB-P8	176.6 \pm 4.6	MB-P8	176.6 \pm 4.6
MC-1	7.254 \pm 0.087	MC-1	7.254 \pm 0.087	ME-6	181.2 \pm 1.9	ME-6	181.2 \pm 1.9
ME-3	7.831 \pm 0.077	ME-3	7.831 \pm 0.077	MB-1	184.8 \pm 2.1	MB-1	184.8 \pm 2.1
MC-2	8.01 \pm 0.10	MC-2	8.01 \pm 0.10	MF-M2	192.9 \pm 1.9	MF-H1	194.7 \pm 1.2
MG-1	8.06 \pm 0.15	MG-1	8.06 \pm 0.15	MF-M1	196.1 \pm 1.7		
ME-4	9.49 \pm 0.12	ME-4	9.49 \pm 0.12	MA-M7	203.1 \pm 1.7	MA-H4	204.0 \pm 1.5
MA-M4	9.84 \pm 0.14	MA-M4	9.84 \pm 0.14	MA-M5	207.3 \pm 3.3		
MH-4	13.805 \pm 0.077	MH-4	13.805 \pm 0.077	MB-6	219.5 \pm 3.8	MB-6	219.5 \pm 3.8
MH-3	14.677 \pm 0.026	MH-3	14.677 \pm 0.026	MB-9	238.0 \pm 3.7		
MI-1	17.01 \pm 0.30	MI-1	17.01 \pm 0.30	MB-3	242.1 \pm 2.8	MB-H1	242.5 \pm 1.2
MH-1	21.795 \pm 0.069	MH-1	21.795 \pm 0.069	MB-P3	246.0 \pm 5.4		
MA-3	39.852 \pm 0.094	MA-3	39.852 \pm 0.094	MC-P7	252.9 \pm 7.9	MC-P7	252.9 \pm 7.9
MK-2	40.9 \pm 1.1	MK-2	40.9 \pm 1.1	MB-5	262.0 \pm 4.4	MB-H2	263.0 \pm 4.2
MB-M6	42.728 \pm 0.062	MB-M6	42.728 \pm 0.062	MB-P7	273 \pm 13		
MJ-1	46.08 \pm 0.26	MJ-1	46.08 \pm 0.26	MB-M5	286.2 \pm 1.5	MB-H3	286.0 \pm 1.5
MA-1	58.15 \pm 0.72	MA-1	58.15 \pm 0.72	MA-M6	304.6 \pm 4.5	MA-M6	304.6 \pm 4.5
ME-1	63.54 \pm 0.44	ME-H1	63.85 \pm 0.24	MC-P8	321.9 \pm 4.0	MC-P8	321.9 \pm 4.0
ME-9	63.98 \pm 0.28			MA-M10	326.6 \pm 5.2	MA-M10	326.6 \pm 5.2
MC-P5	66.41 \pm 0.86	MC-P5	66.41 \pm 0.86	MF-1	333 \pm 20	MF-1	333 \pm 20
MA-8	71.72 \pm 0.48			MB-M1	336 \pm 17		
MC-P6	71.79 \pm 0.83	MC-P6	71.79 \pm 0.83	MB-7	336.3 \pm 6.8	MB-H4	341.7 \pm 2.3
MA-7	72.09 \pm 0.56	MA-H1	71.87 \pm 0.36	MB-M3	340 \pm 14		
MD-1	72.37 \pm 0.43	MD-1	72.37 \pm 0.43	MB-4	342.6 \pm 2.5		
MD-P4	73.77 \pm 0.41	MD-P4	73.77 \pm 0.41	MB-P1	359 \pm 13	MB-P1	359 \pm 13
MC-P4	74.33 \pm 0.96	MC-P4	74.33 \pm 0.96	MF-2	375 \pm 12	MF-2	375 \pm 12
MD-P3	75.47 \pm 0.49	MD-P3	75.47 \pm 0.49	*MB-M8	377.5 \pm 3.6	MB-H5	379.9 \pm 3.1
MB-P4	79 \pm 14	MB-P4	79 \pm 14	*MB-P2	383.4 \pm 7.0		
MA-M8	81.58 \pm 0.33	MA-H2	81.62 \pm 0.29	*MB-8	403 \pm 14	MB-H6	405.8 \pm 4.2
MA-M9	81.85 \pm 0.69			*MB-M4	406.1 \pm 4.4		
MA-M1	82.51 \pm 0.23	MA-H3	82.45 \pm 0.22	*MB-M7	421.8 \pm 5.7	MB-H7	419.2 \pm 3.5
MA-9	86.3 \pm 1.1	MA-9	86.3 \pm 1.1	MB-2	467.0 \pm 9.2	MB-2	467.0 \pm 9.2
MA-M2	91.7 \pm 1.3	MA-M2	91.7 \pm 1.3	MB-M9	529 \pm 15	MB-M9	529 \pm 15
MA-M11	106.91 \pm 0.39	MA-M11	106.91 \pm 0.39				

overlapping date is included in both summations. However, this situation typically occurs when the overlapping age has large errors and its contribution to the two new Gaussians will be minor; therefore, it represents a more objective approach compared with artificially combining a date with either of two overlapping dates.

Gaussian fusion produces a new distribution with a reduced variance, artificially inflating the peak height and therefore its statistical significance relative to expected exponential baseline. However, this increase in significance is countered by the reduction in the number of stalagmites, which increases the chance of any peak being random. We find that in practice Gaussian fusion of overlapping U–Th ages reduces the significance of the peak height, and is therefore a conservative option for determining any potential climatic influences.

The removal of potential duplicates results in a total of 63 specimens (Table 1). Again, the number of stalagmites increases to the present day, and their distribution through time is best described by an exponential curve (Fig. 3b). The correlation between the data and the exponential function fit to the data is statistically significant in both cases, with smaller p-values in the combined data set than in the raw (Table 2).

3.1. Potential biases in the data

The interpretation of the frequency distribution of ages in terms of environmental change necessarily assumes that the samples were collected at random in each of the 13 caves. However, to what extent is this assumption valid?

Dates from drill cores or powders will always tend to underestimate the onset of stalagmite growth because it is difficult to drill the very base of a stalagmite and the positioning of rocks, slopes and other obstacles can make access problematic. Furthermore, there is no certainty of removing only material from the central growth axis as sampling from the flanks of the stalagmites will introduce younger material. Such biases may increase the uncertainty of the timing of any climatic events. As a result, information regarding leads and lags in the system cannot be reliably obtained from this method. Another factor to consider is that stalagmites have not been sampled in a true random fashion. Stalagmite inaccessibility will prevent 100% coverage of all stalagmites in a cave because of location, specimen fragility, and human bias, among other factors.

Although it is unlikely that any of these caveats have a significant or systematic bias that influence a stalagmite age by more than a thousand years or so, the significance of the exponential relationship will be reduced if any bias is introduced. The presence of a statistically robust exponential relationship ($p = 0.08$) occurs despite these potential biases (Table 2).

We further investigated the potential of human bias by assessing the distribution of stalagmite ages in each of the two field seasons. During the initial visits it is difficult to estimate the ages of stalagmites by their appearance. However, once the mini-core U–Th ages are known, populations of stalagmites with desirable ages can be targeted for more sampling in subsequent field seasons. Therefore, the age determinations for the 31 stalagmites sampled during the first field season in 2009 are as close to a random sample of the population as possible. Nevertheless, the 2009 suite of basal ages does contain a disproportionately large number of Holocene stalagmites relative to the distribution of ages

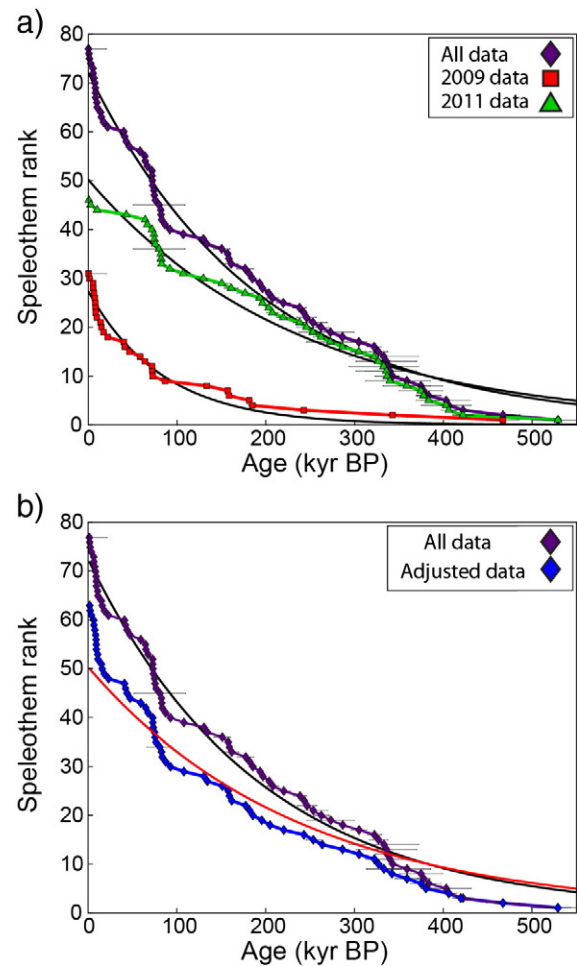


Fig. 4. Cumulative frequency of stalagmite ages over the last ~530 ka in 13 caves in southwest Sulawesi. a) All 77 stalagmites are shown in the purple curve. Red indicates the 31 samples from the 2009 field-season. Green indicates the 46 samples from the 2011 field-season. The best-fit exponential relationship for each data set is shown in black. b) Comparison of the cumulative frequency curves for all 77 stalagmites (purple with black exponential curve) versus the adjusted set of 63 stalagmites (blue with red exponential curve) after accounting for potential duplication of single drip sites. The significance of each exponential curve is indicated in Table 2.

in the full data set (Fig. 4a). The data set may be over-representative of younger specimens because the upper galleries in caves with older material are much harder to reach, whereas younger stalagmites are easy to find on the present-day floor of a cave. Despite this bias Lilliefors test results in Table 2 indicate that the age distribution of the 2009 suite is highly exponential (99% confidence).

During the 2011 field season we were able to use the first suite of basal U–Th ages to determine the general appearance characteristics of younger or older stalagmites in terms of relative cleanliness, style of crusts and height in the cave. This prior knowledge introduced an obvious human bias in sampling 46 relatively old stalagmites during the 2011 expedition (Fig. 4a). As a result, the basal ages for the 2011 data set show a reduced significance for an exponential distribution (95% confidence). Because the two biases in 2009 and 2011 are inconsistent, the full data set has a reasonably random distribution that defines a robust exponential basal age distribution (90% likely to be exponential, Table 2) after accounting for over-representation of individual flow routes in single caves.

We do not necessarily expect individual caves to always show an ideal exponential relationship in the age distribution of stalagmites.

Table 2
Lilliefors test of the exponential relationship for each stalagmite basal-age data set.

Data set	No. of samples	p-Value	Confidence in exponential
2009 data	31	0.01	99%
2011 data	46	0.02	95%
Adjusted data	63	0.08	90%
All data	77	0.12	85%

Individual caves are subject to localised natural events, including the erosion of new floor levels, cave collapse and stream re-routing. By sampling a population of different caves with stalagmites encompassing the last ~530 kyr we sought to average out these major events as part of the observed natural attrition. Populations of stalagmites over a wide area provide the most robust record of natural attrition. As a result the greater the number of caves studied in an area, the more reliable are the obtained results.

4. Discussion

To explain the observed distribution of speleothem ages through time, we have introduced a simple model for exploring stalagmite natural attrition and variable growth phases. This model is applicable to the Sulawesi data set as well as to the data presented below for Korea (Jo et al., 2014) and Australia (Ayliffe et al., 1998).

4.1. Natural attrition of stalagmites

Processes in which independent events occur at a constant average probability produce an exponential relationship with time (e.g., radioactive decay). Stalagmite basal ages represent the surviving fraction of an original population. The first-order exponential age-frequency distribution of stalagmites in southwest Sulawesi can be explained by processes of stalagmite attrition occurring at a near-constant rate over 100-kyr scales. Therefore, in a hypothetical cave system where environmental conditions are in long-term steady state, sampling all stalagmites would produce an exponential relationship, with new material created at a near-constant rate and older material lost through processes of attrition. Because the first-order age distribution approximates an exponential relationship, the probability of any individual stalagmite being destroyed (not the same as cessation of growth) or buried must also be generally constant over the ~500-kyr timescale examined in this study.

Sources of stalagmite loss include downward erosion of the karst terrain, cave collapse, in-cave erosional processes, in-cave sedimentation and speleothem precipitation covering stalagmites (Gilli, 2004), stalagmite dissolution by water undersaturated with calcite, earthquakes (Becker et al., 2006) and cave ice (Kempe, 2004). Certain cyclical attritional behaviour may be present, such as that which might result from fluctuating climatic conditions. However, such behaviour is averaged over ~100-kyr scales such that the overall distribution approximates a constant rate.

Fig. 6 shows the relative probability of stalagmite growth in the southwest Sulawesi caves over the last ~530 kyr. To account for uncertainties in individual U–Th ages, the age distributions (assumed to be Gaussian) for the 63 stalagmites in the adjusted data set were summed in 5 kyr increments (e.g., as in Gordon and Smart, 1984). This is the optimal increment size to ensure that stalagmites of similar age are grouped whilst maintaining sufficient temporal resolution for the record. The significance of the peaks is highly dependent on increment size because of the statistical uncertainty created by assigning an event (beginning of stalagmite growth) to a continuous age distribution. Larger increments reduce the certainty of the location of a peak but increase the significance of peaks therein. Smaller increment sizes produce less significant but more accurately located peaks.

A comparison of the Sulawesi record with similar records from Korea (Jo et al., 2014) and South Australia (Ayliffe et al., 1998) suggests that the exponential relationship of the age distribution of stalagmites is likely to be a general cave phenomenon occurring at rates intrinsic to each geographical location. The U–Th age distribution of speleothems from Korea shows a clear exponential function for the last 530 kyr (Fig. 5a). Speleothem U–Th data for South Australia do not show a full exponential relationship in the absence of Holocene stalagmites under dry Holocene conditions (Fig. 5c). However, the exponential relationship is clear from 550 to 20 ka. Peaks in stalagmite growth frequency

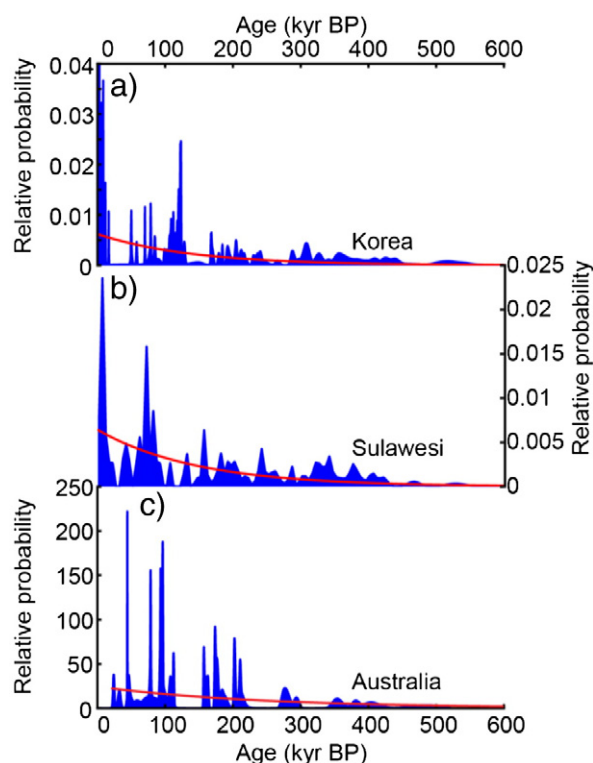


Fig. 5. Probability of stalagmite growth at three locations determined from the frequency of U–Th ages: a) Korea (Jo et al., 2014, with Holocene data truncated), b) Sulawesi (this study), and c) Australia (Ayliffe et al., 1998). The Korean and Australian records are determined from U–Th dates on stalagmite slabs, whereas the Sulawesi data are from basal mini-core U–Th dates only. Red curves define the exponential relationship in Korea, Sulawesi and Australia.

that occurred during Marine Isotope Stages (MIS) 3 and 4 are twice as high as peaks during MIS 6 which, in turn, are twice as high as peaks from MIS 8, and so on through MIS 10 and MIS 12. This result indicates that the peaks in the age frequency distribution during relatively wet periods define the exponential relationship better than the troughs because of the higher data density and better counting statistics. The large spatial scale of this relationship validates the use of stalagmite growth frequency as a useful palaeoclimatic indicator, particularly of wetter intervals (e.g., Ayliffe et al., 1998; Jo et al., 2014).

That the Sulawesi basal age derived growth frequency record is comparable to the full growth frequency records of Korea and South Australia suggests that the basal age approach employed here is an acceptable approximation of growth frequency. Whilst top ages and detailed age models will increase the accuracy of a growth frequency record they will incur additional damage to the cave environment.

The goal of many stalagmite palaeoclimate studies is the production of a continuous record covering the available time span of speleothem growth. Due to the natural asymmetry in the distribution of ages, a random sampling of stalagmites is unlikely to produce a continuous record over the depositional period unless a very large number of specimens are taken. This would involve significant wastage of younger specimens and the unnecessary degradation of cave conditions for future generations. Sampling strategies must be designed to account for this asymmetry. Mini-coring over successive field-seasons, as described here, represents a good practice for the collection of high-quality stalagmites and preservation of caves in their natural state.

Previous studies have interpreted the relatively high number of young stalagmites as a period of increased growth frequency because of warmer and/or wetter Holocene climates (Vaks et al., 2013) or sampling bias (Williams et al., 2010). However, the exponential relationship caused by natural attrition in stalagmite populations described here

indicates that a more statistically robust technique can be used to prove such claims. The predictable distribution of stalagmite ages caused by natural attrition allows this relationship to be removed from the data to reveal second-order changes in stalagmite growth frequency through time.

4.2. Deviations from the idealised exponential relationship

There are three methods by which second-order deviations from idealised exponential relationships can occur: 1) Destructive processes that target stalagmites of a certain age. 2) Non-steady state creation of new stalagmites. 3) Statistical fluctuations due to limited sample size.

4.2.1. Discriminant destructive processes

Whilst most processes of stalagmite attrition will act indiscriminately upon the entire stalagmite population, some processes do act discriminately: Downward erosion of karst terrains will disproportionately destroy stalagmites located in the older, upper chambers and lead to a maximum age of the stalagmite population. This will influence the shape of the idealised exponential relationship but is unlikely to produce deviations. Therefore, deviations from the expected relationship represent changes in the frequency of stalagmite creation caused by other factors.

4.2.2. Non-steady state creation of new stalagmites

Fluctuations in stalagmite growth frequency are well recognised in the literature and generally interpreted as resulting from changing climate (e.g., Hennig et al., 1983; Gordon et al., 1989; Baker et al., 1993; Ayliffe et al., 1998; Wang et al., 2004; Vaks et al., 2006; Vaks et al., 2010; Vaks et al., 2013). Under this scenario, periods of increased stalagmite growth initiation reflect times of greater water mobility, soil CO₂ production and dissolution of the limestone host rock (e.g., Baker et al., 1993). In the tropics, where glacial–interglacial temperature changes are subdued (Visser et al., 2003), rainfall amount is likely to be the primary factor influencing stalagmite growth. Stalagmite growth frequencies exceeding the expected number may indicate wetter climatic conditions that promote stalagmite growth, whereas fewer stalagmites may reflect drier climates.

Knowledge of the first-order exponential relationship can be used to assess the record in a more statistically robust way. By removing the exponential baseline, the relative heights of the peaks in stalagmite growth can be compared on a common baseline (Fig. 6). To ensure that the results are not similar to what could be generated by sampling 63 random data points from the same exponential relationship, 10,000 synthetic ages were calculated from the same exponential relationship to determine the predicted variation through time caused by chance. This process allows the data to be normalised to unit variance and levels of significance to be attached to peaks (Fig. 6c).

We identified several peaks in stalagmite growth (425–400, 385–370, 345–335, 330–315, 160–155, 75–70 and 10–5 ka) when the frequency of growth initiation exceeds two standard deviations above the exponential relationship, with troughs between peaks below one standard deviation. These peaks indicate wetter than average climates. The increasing apparent duration of the wet peaks further back in time likely results from the increasing age error rather than longer wet periods. The growth probability distribution is skewed towards peaks with frequent stalagmite growth (Fig. 6c), thus making it statistically impossible to determine dry periods from this record (at times when only one or two stalagmites are predicted).

4.2.3. Limitations of sample size

An idealised exponential curve would be produced by an infinite number of stalagmites growing under steady state conditions. Under non-steady state conditions deviations from this curve would also be defined best by an infinite number of stalagmites. In speleothem growth frequency studies larger sample sizes improve the counting statistics and mute any potential human bias. Heremann (2000) suggests a minimum number of 150 dates to produce a reliable growth frequency curve – however this is using all stalagmite ages and 150 dates would likely represent fewer than the 63 stalagmites used here, increasing the chances of non-climatic cave events being recorded.

Increasing the number of stalagmites also increases the precision of any interpretations. The suite of 63 stalagmites from Sulawesi provides statistically robust peaks at the 5 kyr bin size. We note that no significant peak in the record is produced by a single specimen. Producing a larger sample size may not be financially viable or take too much time out of other worthwhile activities in the cave. Excessive sampling may

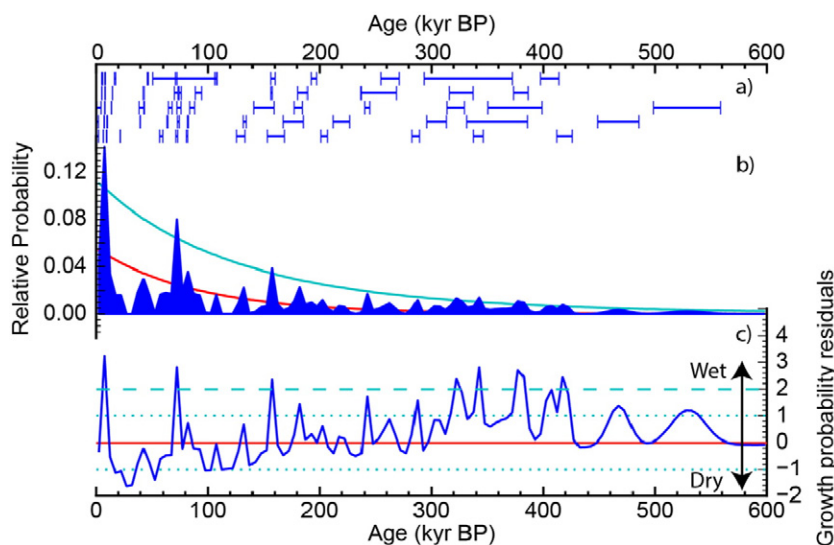


Fig. 6. Climatic influence on stalagmite growth since ~530 ka in 13 caves in southwest Sulawesi. a) Ages for the adjusted set of 63 stalagmites are shown with 2σ error bars (blue). b) Relative probability of stalagmite growth based on summing individual age distributions for each sample (assuming Gaussian age errors) within 5 kyr increments. Red line indicates the baseline exponential relationship, and the cyan line indicates $+2\sigma$ variation. c) Distribution of growth probability residuals (standardised to unit variance) after subtraction of the baseline exponential relationship. Dotted and dashed cyan lines show $\pm 1\sigma$ and $\pm 2\sigma$ unit variance. Positive residuals that exceed the 2σ value reflect significant increases in the onset of stalagmite growth related to increases in rainfall.

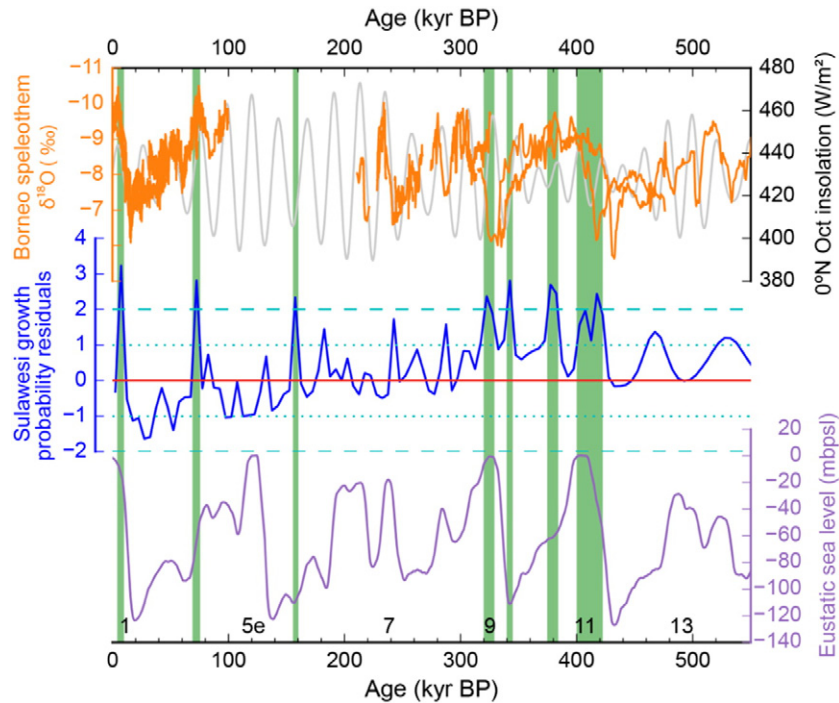


Fig. 7. Comparison of stalagmite growth in Sulawesi with speleothem $\delta^{18}\text{O}$ records for Borneo and eustatic sea level. The distribution of stalagmite growth probability residuals (blue) for 13 caves in southwest Sulawesi compared with Borneo $\delta^{18}\text{O}$ records (orange; Partin et al., 2007; Meckler et al., 2012; Carolin et al., 2013) and 0°N October insolation (grey). Eustatic sea level (purple) is shown for reference (Bintanja and van de Wal, 2008). Interglacial marine isotope stages are numbered at the base. Green bars link $>2\sigma$ peaks in Sulawesi stalagmite growth.

also contribute to some cave aesthetic deterioration but drill holes can be sited on the side of the stalagmite away from the view to lessen the visual impact.

A similar approach can be taken with the number of cave sites sampled, which should all be under the same climatic regime. The larger the number of caves sampled, the more the influence of cave specific irregular events such as changes in cave morphology are averaged, increasing the influence of climatic changes. In theory the observed relationship seen in the stalagmites should be reflected in the number of caves displaying stalagmites of a certain age – we would expect the exponential relationship to exist here to, if a sufficient number of stalagmite basal ages were taken.

4.3. Sulawesi stalagmite growth and rainfall

The timing of a prominent cluster of three statistically significant peaks in stalagmite growth in Sulawesi (425–400, 385–370, 345–335 ka) corresponds to a prolonged wet period recorded by lower $\delta^{18}\text{O}$ values in stalagmites from Borneo (Fig. 7; Meckler et al., 2012). This prolonged wet period is coincident with a period of low precessional variability (Meckler et al., 2012). The accompanying high-frequency stalagmite growth in Sulawesi indicates that this wet anomaly had a regional climatic footprint.

The Sulawesi record also shows that peaks in stalagmite growth initiation generally correspond with relatively wet conditions during interglacials. The first of these wet periods (425–400 ka) is coincident with interglacial conditions at MIS 11. A wet period at 330–315 kyr is synchronous with MIS 9, and the most recent interglacial (MIS 1) also corresponds to a period of stalagmite growth at 10–5 ka. Wet anomalies in the Indonesian maritime continent region during interglacial periods are expected because previous studies suggest that rising sea levels led to increased rainfall through increased deep convective activity caused by larger sea surface area and higher SSTs (e.g., De Deckker et al., 2002; Griffiths et al., 2009; DiNezio et al., 2011; Meckler et al., 2012; DiNezio and Tierney, 2013).

Speleothem $\delta^{18}\text{O}$ records indicate wet anomalies throughout the maritime continent region in the Holocene (e.g., Partin et al., 2007; Griffiths et al., 2009; Ayliffe et al., 2013; Carolin et al., 2013) and in previous interglacials (Meckler et al., 2012), yet there is a deficit of speleothem material for MIS 5e. The new Sulawesi record repeats this pattern, with a wet anomalies occurring in MIS 11, 9 and 1 but apparently dry conditions during MIS 5e (Fig. 7). The absence of MIS 5e stalagmite growth appears to extend to the adjacent mid-latitudes, in South Australia (Ayliffe et al., 1998) and Korea (Jo et al., 2014) (Fig. 6).

The apparent drying trend in the Sulawesi record over the last 400 kyr is due to a limited sample size and the increasing spread of the ages with increasing age, which combine to increase the probability of growth at times without stalagmite growth. In contrast, the amplitudes of the wet intervals, represented by more stalagmite growth, do not show a significant trend towards the present. The infrequency of significant peaks in stalagmite growth likely reflects the small population size used in this study, rather than the presence of lengthy dry periods on Sulawesi. Nevertheless, three significant peaks in growth frequency occur at 160–155 ka, 75–70 ka and 10–5 ka. The peaks at 75–70 ka and 10–5 ka in Sulawesi correspond to lower $\delta^{18}\text{O}$ (wetter) intervals recorded in stalagmites from Borneo spanning ~100–0 ka (Fig. 7; Partin et al., 2007; Carolin et al., 2013), confirming regional scale increases in precipitation at these times.

The wet period at 75–70 ka occurred during an intermediate sea level and is thought to be related to either broad meridional ITCZ forcing of monsoon rainfall (e.g., Wang et al., 2001; Wang et al., 2008; Ayliffe et al., 2013) or to the effect of ENSO forcing on deep atmospheric convection over the maritime continent region (e.g., Partin et al., 2007; Meckler et al., 2012; Carolin et al., 2013). The 10–5 ka peak in the Sulawesi record marks the start of the current interglacial when rising sea levels are thought to have led to increased convective rainfall activity (De Deckker et al., 2002; Griffiths et al., 2009; DiNezio et al., 2011; Meckler et al., 2012; Denniston et al., 2013; DiNezio and Tierney, 2013). The opening of the Karimata Strait also provided a large freshwater flux to the region that may have had a significant impact on SSTs and

rainfall (De Deckker et al., 2002; Linsley et al., 2010; Griffiths et al., 2012).

5. Conclusions

We have shown that the distribution of stalagmites that survive to the present day shows a previously unrecognised first-order exponential relationship. This suggests that the combined effect of karst processes that govern the natural attrition of stalagmites is generally near-constant on > 100 kyr scales. Natural attrition of stalagmite populations is driven by downwards erosion, cave-collapse, burial of older material, dissolution by undersaturated groundwater and other weathering and erosional processes. In Sulawesi, and elsewhere, the result of these processes of natural attrition creates an exponential relationship of stalagmite basal ages over the last ~500 kyr.

Peaks in the frequency of stalagmite growth initiation are likely to result from warmer, wetter conditions. By accounting for natural attrition, a better comparison can be made of the relative peak heights through time than was previously possible using stalagmite growth frequency curves that have not been corrected for natural attrition.

Our results provide initial insights into the Late Quaternary palaeoclimate history of Sulawesi. We have shown that peaks in stalagmite growth frequency over the last ~530 kyr correspond to wet periods in Borneo, thus confirming regional precipitation as the likely cause and demonstrating the suitability of this technique for retrieving basic palaeoclimate information. Stalagmite dating studies cannot match the temporal resolution of detailed palaeoclimate studies, but analysis of stalagmite growth initiation can provide valuable first-order palaeoclimate information well in advance.

Our approach utilises the ages of low-impact mini-cores extracted in situ from the bases of stalagmites, thus leaving the intrinsic value of the cave intact. The collection of stalagmites for scientific research must be carefully targeted to avoid oversampling of more recent periods and the unnecessary removal of stalagmites, which damages the cave condition. The mini-coring techniques used in this study would be easy to implement in caves requiring special protection, such as show caves, and in those with cultural significance or outstanding scenic value.

Supplementary data to this article can be found online at <http://dx.doi.org/10.1016/j.palaeo.2015.10.030>.

Acknowledgements

We would like to thank David Heslop for his help with the statistics and for providing insight into the early versions of this paper. We thank the Indonesian Institute of Sciences (LIPI) for logistical support, Engkos Kosasih, Djupriono, and the staff of Bantimurung-Bulusaraung National Park (with special thanks to Saiful) for assistance in the field during the 2009 and 2011 expeditions. We are particularly grateful to Neil Anderson, Dan Zwartz, Garry Smith and Bambang Suwargadi, who provided expertise in cave conservation and technical assistance. The work was conducted in Indonesia under Kementerian Negara Riset dan Teknologi (RISTEK) research permit numbers 04/TKPIPA/FRP/SM/IV/2009 and 1b/TKPIPA/FRP/SM/I/2011. Financial support for the research was provided by the Australian Research Council Discovery grants DP0663274 and DP1095673 to M.K.G., W.S.H., J.-x.Z., J.C.H., R.L.E. and H.C.; and the National Natural Science Foundation of China grant NSFC-41230524 to H.C. U-Th dating at the HISPEC was supported by the ROC MOST and NTU grants (102-2116-M-002-022, 103-2119-M-002-022, and 101R7625) to CCS.

References

Acker, J.G., Leptoukh, G., 2007. Online analysis enhances use of NASA earth science data. *Eos. Trans. AGU* 88, 14–17.

Atkinson, T.C., 1983. Growth mechanisms of speleothems in Castleguard Cave, Columbia Icefields, Alberta, Canada. *Arct. Alp. Res.* 15, 523–536.

Ayliffe, L.K., Marianelli, P.C., Moriarty, K.C., Wells, R.T., McCulloch, M.T., Mortimer, G.E., Hellstrom, J.C., 1998. 500 ka precipitation record from southeastern Australia: evidence for interglacial relative aridity. *Geology* 26, 147–150.

Ayliffe, L.K., Gagan, M.K., Zhao, J.-X., Drysdale, R.N., Hellstrom, J.C., Hantoro, W.S., Griffiths, M.L., Scott-Gagan, H., Pierre, E.S., Cowley, J., Suwargadi, B.W., 2013. Rapid interhemispheric climate links via the Australasian monsoon during the last deglaciation. *Nat. Commun.* 4, 2908. <http://dx.doi.org/10.1038/ncomms3908>.

Baker, A., Genty, D., 1998. Environmental pressures on conserving cave speleothems: effects of changing surface land use and increased cave tourism. *J. Environ. Manag.* 53, 165–175.

Baker, A., Smart, P.L., Ford, D.C., 1993. Northwest European palaeoclimate as indicated by growth frequency variations of secondary calcite deposits. *Palaeogeogr. Palaeoclimatol. Palaeoecol.* 100, 291–301.

Becker, A., Davenport, C.A., Eichenberger, U., Gilli, E., Jeannin, P.-Y., Lacave, C., 2006. Speleoseismology: a critical perspective. *J. Seismol.* 10, 371–388.

Bintanja, R., van de Wal, R.S.W., 2008. North American ice-sheet dynamics and the onset of 100,000-year glacial cycles. *Nature* 454, 869–872.

Brown, D.H., 2011. *Archaeological Archives. A Guide to Best Practice in Creation, Compilation, Transfer and Curation*. Institute for Archaeologists, Reading 0948393912.

Calaforra, J.M., Fernandez-Cortés, A., 2003. Environmental control for determining human impact and permanent visitor capacity in a potential show cave before tourist use. *Environ. Conserv.* 30, 160–167.

Carolin, S.A., Cobb, K.M., Adkins, J.F., Clark, B., Conroy, J.L., Lejau, S., Malang, J., Tuen, A.A., 2013. Varied response of Western Pacific hydrology to climate forcings over the Last Glacial Period. *Science* 340, 1564–1566.

Cheng, H., Edwards, R.L., Shen, C.-C., Polyak, V.J., Asmerom, Y., Woodhead, J., Hellstrom, J.C., Wang, Y., Kong, X., Spötl, C., Wang, X., Calvin Alexander, E., Jr., 2013. Improvements in ^{230}Th dating, ^{230}Th and ^{234}U half-life values, and U-Th isotopic measurements by multi-collector inductively coupled plasma mass spectrometry. *Earth Planet. Sci. Lett.* 371–372, 82–91.

Cigna, A.A., Burri, E., 2012. Development, management and economy of show caves. *Int. J. Speleol.* 29B, 1–27.

Cruz, F.W., Burns, S.J., Karmann, I., Sharp, W.D., Vuille, M., Cardoso, A.O., Ferrari, J.A., Dias, P.L.S., Viana, O., 2005. Insolation-driven changes in atmospheric circulation over the past 116,000 years in subtropical Brazil. *Nature* 434, 63–66.

Dai, A., Wigley, T.M.L., 2002. Global patterns of ENSO-induced precipitation. *Geophys. Res. Lett.* 27, 1283–1286.

De Deckker, P., Tapper, N., van der Kaars, S., 2002. The status of the Indo-Pacific Warm Pool and adjacent land at the Last Glacial Maximum. *Glob. Planet. Chang.* 35, 25–35.

Denniston, R.F., Wyrwoll, K.-H., Asmerom, Y., Polyak, V.J., Humphreys, W.F., Cugley, J., Woods, D., LaPointe, Z., Peota, J., Greaves, E., 2013. North Atlantic forcing of millennial-scale Indo-Australian monsoon dynamics during the Last Glacial period. *Quat. Sci. Rev.* 72, 159–168.

DiNezio, P.N., Tierney, J.E., 2013. The effect of sea level on glacial Indo-Pacific climate. *Nat. Geosci.* 6, 485–491.

DiNezio, P.N., Clement, A., Vecchi, G.A., Soden, B., Broccoli, A.J., Otto-Bliesner, B.L., Braconnot, P., 2011. The response of the Walker circulation to Last Glacial Maximum forcing: implications for detection in proxies. *Paleoceanography* 26, PA3217.

Dorale, J.A., Gonzalez, L.A., Reagan, M.K., Pickett, D.A., Murrell, M.T., Baker, R.G., 1992. A high-resolution record of Holocene climate change in speleothem calcite from Cold Water Cave, Northeast Iowa. *Science* 258, 1626–1630.

Draxler, R.R., Rolph, G.D., 2012. HYSPLIT-Hybrid Single-Particle Lagrangian Integrated Trajectory Model. <http://www.arl.noaa.gov/ready/hysplit4.html> (accessed 4.23.12).

Fairchild, I.J., Baker, A., 2012. Archiving speleothems and speleothem data. *Speleothem Science: From Process to Past Environment*. Blackwell Publishing Ltd.

Frappier, A.B., 2008. A stepwise screening system to select storm-sensitive stalagmites: taking a targeted approach to speleothem sampling methodology. *Quat. Int.* 187, 25–39.

Gascoyne, M., Schwarz, H.P., Ford, D.C., 1983. Uranium-series ages of speleothem from northwest England: correlation with Quaternary climate. *Philos. Trans. R. Soc.* B 301, 143–164.

Genty, D., Blamart, D., Quahdi, R., Gilmour, M., Baker, A., Jouzel, J., Van-Exter, S., 2003. Precise dating of Dansgaard-Oeschger climate oscillations in western Europe from stalagmite data. *Nature* 421, 833–837.

Geyh, A.M., 1970. Zeitliche Abgrenzungen von Klimaänderungen mit C-14 Daten. *Beih. Geol. Jahrb.* 98, 15–22.

Gilli, E., 2004. Glacial causes of damage and difficulties to use speleothems as palaeoseismic indicators. *Geodin. Acta* 17, 229–240.

Gordon, D., Smart, P.L., 1984. Comments on “Speleothems, travertines, and paleoclimates” by G. J. Hennig, R. Grün, and K. Brunnacker. *Quat. Res.* 22, 144–147.

Gordon, D., Smart, P.L., Ford, D.C., Andrews, J.N., Atkinson, T.C., Rowe, P.J., Christopher, N.S.J., 1989. Dating of late Pleistocene interglacial and interstadial periods in the United Kingdom from speleothem growth frequency. *Quat. Res.* 31, 14–26.

Griffiths, M.L., Drysdale, R.N., Gagan, M.K., Zhao, J.-x., Ayliffe, L.K., Hellstrom, J.C., Hantoro, W.S., Frisia, S., Feng, Y.-x., Cartwright, I., St. Pierre, E., Fischer, M.J., Suwargadi, B.W., 2009. Increasing Australian-Indonesian monsoon rainfall linked to early Holocene sea-level rise. *Nat. Geosci.* 2, 636–639.

Griffiths, M.L., Drysdale, R.N., Gagan, M.K., Zhao, J.-X., Hellstrom, J.C., Ayliffe, L.K., Hantoro, W.S., 2012. Abrupt increase in east Indonesian rainfall from flooding of the Sunda Shelf 9500 years ago. *Quat. Sci. Rev.* 74, 273–279.

Hellstrom, J., 2003. Rapid and accurate U/Th dating using parallel ion-counting multi-collector ICP-MS. *J. Anal. At. Spectrom.* 18, 1346–1351.

Hellstrom, J., 2006. U-Th dating of speleothems with high initial ^{230}Th using stratigraphical constraint. *Quat. Geochronol.* 1, 289–295.

Hennig, G.J., Grün, R., Brunnacker, K., 1983. Speleothems, travertines, and paleoclimates. *Quat. Res.* 20, 1–29.

- Hermann, H., 2000. Reconstruction of paleoclimatic changes in central Europe between 10 and 200 thousand years BP, based on analysis of growth frequency of speleothems. *Studia Quaternaria* 17, 35–70.
- Jo, K.-n., Woo, K.S., Yi, S., Yang, D.Y., Lim, H.S., Wang, Y., Cheng, H., Edwards, R.L., 2014. Mid-latitude interhemispheric hydrologic seesaw over the past 550,000 years. *Nature* 508, 378–382.
- Kempe, S., 2004. Natural speleothem damage in Postojnska Jama (Slovenia), caused by glacial cave ice? A first assessment. *Acta Cardiol.* 33 (1), 265–289.
- Linsley, B.K., Rosenthal, Y., Oppo, D.W., 2010. Holocene evolution of the Indonesian throughflow and the western Pacific warm pool. *Nat. Geosci.* 3, 578–583.
- McDonnell, T., 2013. Slicing open stalagmites to reveal climate secrets: climate desk. <http://climatedesk.org/2013/06/slicing-open-stalagmites-to-reveal-climate-secrets/> (accessed 9.9.13).
- Meckler, A.N., Clarkson, M.O., Cobb, K.M., Sodemann, H., Adkins, J.F., 2012. Interglacial hydroclimate in the tropical west Pacific through the Late Pleistocene. *Science* 336, 1301–1304.
- Mickler, P.J., Ketcham, R.A., 2004. Application of high-resolution X-ray computed tomography in determining the suitability of speleothems for use in paleoclimatic, paleohydrologic reconstructions. *J. Cave Karst Stud.* 6, 4–8.
- Partin, J.W., Cobb, K.M., Adkins, J.F., Clark, B., Fernandez, D.P., 2007. Millennial-scale trends in west Pacific warm pool hydrology since the Last Glacial Maximum. *Nature* 449, 452–455.
- Šebela, S., Turk, J., 2014. Sustainable use of the Predjama Cave (Slovenia) and possible scenarios related to anticipated major increases in tourist numbers. *Tour. Manag. Perspect.* 10, 37–45.
- Shen, C.-C., Lawrence Edwards, R., Cheng, H., Dorale, J.A., Thomas, R.B., Bradley Moran, S., Weinstein, S.E., Edmonds, H.N., 2002. Uranium and thorium isotopic and concentration measurements by magnetic sector inductively coupled plasma mass spectrometry. *Chem. Geol.* 185, 165–178.
- Shen, C.-C., Wu, C.C., Cheng, H., Edwards, R.L., Hsieh, Y.-T., Gallet, S., Chang, C.C., Li, T.Y., Lam, D.D., Kano, A., Hori, M., Spotl, C., 2012. High-precision and high-resolution carbonate ^{230}Th dating by MC-ICP-MS with SEM protocols. *Geochim. Cosmochim. Acta* 99, 71–86.
- Spötl, C., Mangini, A., 2007. Speleothems and paleoglaciators. *Earth Planet. Sci. Lett.* 254, 323–331.
- Spötl, C., Matthey, D., 2012. Scientific drilling of speleothems – a technical note. *Int. J. Speleol.* 41, 29–34.
- Vaks, A., Bar-Matthews, M., Ayalon, A., Matthews, A., Frumkin, A., Dayan, U., Halicz, L., Almogi-Labin, A., Schilman, B., 2006. Paleoclimate and location of the border between Mediterranean climate region and the Saharo–Arabian Desert as revealed by speleothems from the northern Negev Desert, Israel. *Earth Planet. Sci. Lett.* 249, 384–399.
- Vaks, A., Bar-Matthews, M., Matthews, A., Ayalon, A., 2010. Late Quaternary paleoclimate of northern margins of the Saharan–Arabian Desert: reconstruction from speleothems of Negev Desert, Israel. *Quat. Sci. Rev.* 29, 2647–2662.
- Vaks, A., Gutareva, O.S., Breitenbach, S.F.M., Avirmed, E., Mason, A.J., Thomas, A.L., Osinzev, A.V., Kononov, A.M., Henderson, G.M., 2013. Speleothems reveal 500,000-year history of Siberian Permafrost. *Science* 340, 183–186.
- Verheyden, S., Genty, D., 2013. Lifting the veil on speleothem sampling. *PAGES News* 21, 5.
- Visser, K., Thunell, R., Stott, L., 2003. Magnitude and timing of temperature change in the Indo-Pacific warm pool during deglaciation. *Nature* 421, 152–155.
- Walczak, I.W., Baldini, J.U.L., Baldini, L.M., McDermott, F., Marsden, S., Standish, C.D., Richards, D.A., Andreo, B., Slater, J., 2015. Reconstructing high-resolution climate using CT scanning of unsectioned stalagmites: a case study identifying the mid-Holocene onset of the Mediterranean climate in southern Iberia. *Quat. Sci. Rev.* 127, 117–128.
- Wang, Y.J., Cheng, H., Edwards, R.L., An, Z., Wu, J., Shen, C.-C., Dorale, J.A., 2001. A high-resolution absolute-dated late Pleistocene monsoon record from Hulu Cave, China. *Science* 294, 2345.
- Wang, X., Auler, A.S., Edwards, R.L., Cheng, H., Cristalli, P.S., Smart, P.L., Richards, D.A., Shen, C.-C., 2004. Wet periods in northeastern Brazil over the past 210 kyr linked to distant climate anomalies. *Nature* 432, 740–743.
- Wang, Y., Cheng, H., Edwards, R.L., Kong, X., Shao, X., Chen, S., Wu, J., Jiang, X., Wang, X., An, Z., 2008. Millennial- and orbital-scale changes in the East Asian monsoon over the past 224,000 years. *Nature* 451, 1090–1093.
- Williams, P.W., Neil, H.L., Zhao, J.-x., 2010. Age frequency distribution and revised stable isotope curves for New Zealand speleothems: palaeoclimatic implications. *Int. J. Speleol.* 39 (2), 99–112.
- Wilson, M.E.J., 2000. Tectonic and volcanic influences on the development and diachronous termination of a Tertiary tropical carbonate platform. *J. Sediment. Res.* 70, 310–324.
- Wilson, M.E.J., Bosence, D.W.J., 1996. The Tertiary evolution of South Sulawesi: a record in redeposited carbonates of the Tonasa Limestone Formation. *Geol. Soc. Lond., Spec. Publ.* 106, 365–389.
- Wilson, M.E.J., Moss, S.J., 1999. Cenozoic palaeogeographic evolution of Sulawesi and Borneo. *Palaeogeogr. Palaeoclimatol. Palaeoecol.* 145, 303–337.